Influence of the mesh dimensions on optically transparent and active antennas at microwaves

Alexis MARTIN, Xavier CASTEL, Mohamed HIMDI, Olivier LAFOND
'Antennes & Dispositifs Hyperfréquences' Department
Institut d'Electronique et de Télécommunications de Rennes (IETR UMR-6164), Université de Rennes 1, Rennes FRANCE

***Abstract* – The paper deals with the study of optically transparent and active square loop coplanar antennas in *X*-band. Frequency tunability of such antennas is provided by a surface mounted beam-lead varactor with micrometric dimensions, thus non-visible to the naked eye. The influence of the mesh dimensions on sheet resistance (from 0.05 Ω/sq to 0.50 Ω/sq), optical transparency (from 66% to 89%) and microwave performance (reflection coefficient, resonance frequency and gain) is evaluated, compared with those of an opaque counterpart and discussed. Design rules for active mesh antennas will conclude the present study.**

***Index Terms* — Optically transparent antennas, active antennas, mesh silver film, frequency tunability, square loop coplanar antennas.**

1. Introduction

Nowadays the development of wireless communications and wireless sensors requires emerging technologies to enhance the communication network performance, especially in dense urban areas. An attractive possibility concerns the development of optically transparent antennas to improve their location in the cities by accessing new surfaces, namely glazed surfaces such as building or car windows. These antennas can be elaborated from transparent and conducting layers printed on glass substrates. The most usual material belongs to the transparent and conducting oxide (TCO) family, namely indium tin oxide (ITO) [1]. Hybrid solutions based on TCO materials and ultrathin metal films are also available such as ITO/Cu/ITO multilayers [2] or AgHT films (ITO/silver multilayer printed on polyester substrate) [3]. Nonetheless ITO is based on a critical raw material (indium).

An alternative solution has been developed specifically at the IETR Laboratory. It is based on mesh metal film printed on glass substrate [4]. Metal layer exhibits low sheet resistance (and low ohmic loss as a result) and apertures inside the metal layer give the needed optical transparency in the visible light spectrum. Metal thickness adjustment prevents any skin depth effect at the working frequency without any change in optical transparency level [4]. Optically transparent passive antennas have been developed from such a material [5], [6].

In this study, we present the influence of the mesh dimensions on the performance of optically transparent active antennas in *X*-band. A previous study has been carried out with a passive antenna made of a wide mesh (pitch value larger than $\lambda_0/30$, with λ_0 the working wavelength) in a microstrip structure [7]. The present work focuses on narrower mesh dimensions (with micrometric size) in a coplanar technology, to study and restrict the mesh influence on the active antenna performance. To this end, three transparent antennas have been fabricated from different mesh dimensions and characterized at microwaves.

2. Antenna Design and Fabrication

The active antenna design is detailed in [8]. It is a square loop coplanar antenna (Fig. 1). The substrate used is a 50.8 mm × 50.8 mm × 0.7 mm 1737 Corning glass substrate with dielectric characteristics $\varepsilon_r = 5.7$ and $tan\delta = 0.006$ at 2 GHz. The conducting layer used is a 2 µm-thick silver film, three times larger than the skin depth thickness (δ=0.64 µm) at 10 GHz.

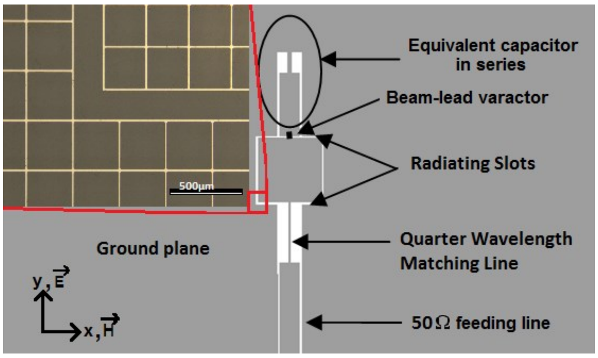

Fig. 1. Geometry of the transparent frequency-agile coplanar antenna. Detail of the mesh silver film in inset.

Three mesh antennas (transparent) and a continuous reference counterpart (opaque) have been fabricated with the process fully described elsewhere [4] from continuous silver film (2 µm-thick) and titanium adhesion ultrathin film (5 nm-thick) deposited by RF sputtering. Subsequently a standard photolithographic wet etching process is used to fabricate the four samples with appropriate photomasks. Stripping of the photoresist leaves the antenna pattern with a periodic array of apertures in the metal coatings for the transparent antenna (inset picture in Fig. 1). The periodic array is characterized by a silver strip width *s* and a pitch *p*. Lastly a MA46580-1209 beam-lead varactor (210 µm × 610 µm) from the M/A-COM Company is soldered with heat-conductive paste. Its capacity value varies from 0.87 pF to 0.17 pF under an external applied DC bias voltage ranging from 2 V to 12 V, respectively. Dimensions are detailed in Table I. Optical transparency in the visible light spectrum and sheet resistance have been computed from (1) and (2), as follows:

$$T\,(\%) = [(p-s)/p]^2 \times T_{sub} \quad (1)$$

$$R_s' = p \times R_s / s \quad (2)$$

and checked with a UV-Visible spectrophotometer and a standard four-probe setup, respectively. T_{sub} is the optical transparency of the bare substrate (0.92 or 92%) and R_s is the sheet resistance of the continuous silver layer (0.008 Ω/sq). Wider the pitch is (for a constant metal strip width), higher the optical transparency level is (from 66% to 89%) and higher the sheet resistance is too (from 0.05 to 0.50 Ω/sq).

TABLE I
Mesh Dimensions and Related Antenna Characteristics

	Antenna 1	Antenna 2	Antenna 3
Pitch p (µm)	100	290	940
Silver strip width s (µm)	15	15	15
Sheet resistance R_s'(Ω/sq)	0.05	0.15	0.50
Optical transparency T (%)	66	83	89

3. Measurements

Numerical simulations have been performed with a continuous silver layer (opaque) using the commercial CST Microwave Studio®. Gain measurements of the three transparent antennas and of the opaque antenna have been carried out in an anechoic chamber from 8 GHz to 12 GHz.

The return loss remains below -10 dB for all antennas and under each biasing value (Fig. 2a). Variation of the resonance frequency under biasing is shown in Fig. 2b. A 400 MHz frequency shift is observed between the narrower mesh antenna 1 and the reference counterpart (4% of the resonance frequency); 800 MHz (8%) between the widest mesh antenna 3 and the reference counterpart. A negligible frequency shift (< 100 MHz) is measured between transparent antennas 1 and 2. Both of these antennas look similar with a working wavelength/pitch ratio equal to $\lambda_0/300$ and $\lambda_0/100$, respectively. Nonetheless, as mentioned in [8], a frequency shift always appears in *X*-band between the mesh antenna and the reference counterpart. And wider the pitch is, higher the shift value is (antenna 3). It is worth noting that this transparent antenna is made from a mesh pattern with a $\lambda_0/30$ ratio value at 10 GHz. These frequency shifts agree with the results presented in [7], whose the narrower mesh used remains close to $\lambda_0/30$ at 24 GHz.

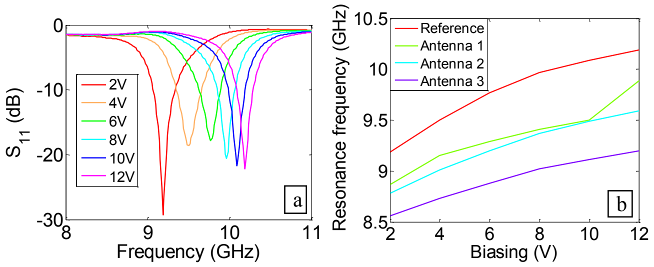

Fig. 2. Variation of the return loss (a) and of the resonance frequency (b) versus biasing.

Radiating patterns have been carried out and gain variation under biasing is shown in Fig. 3. Due to diffraction effect on sample edges, ripples superimpose on the radiation patterns (they are not shown for brevity). Thus the gain is an average value between the maximum value of the ripple and the gain on axis. A value close to 0.5 dBi is obtained for the reference antenna. A 2 dB lower gain is reached with antenna 1, and 0.5 dB less with antenna 2. Despite a negligible effect of the mesh dimensions on the resonance frequency values of the antennas 1 and 2, the use of a wider pitch induces an increase of the sheet resistance (Table I), and thus of the ohmic loss. This behavior is fully confirmed by the mesh antenna 3 performance. However transparent antennas made from such a material exhibit high microwave performance compared with those made from ultrathin metal, TCO or hybrid solutions [2].

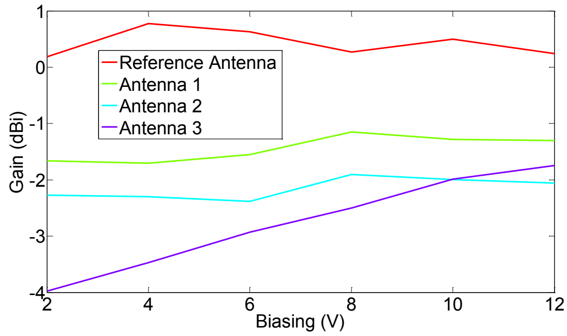

Fig. 3. Gain variation versus biasing.

4. Conclusion

The influence of the mesh dimensions on the microwave performance of optically transparent and active antennas in *X*-band has been evaluated and discussed. This study leads to some design rules. A mesh pattern with a pitch close to $\lambda_0/100$ at the working frequency is the best tradeoff: a high optical transparency (83%) is reached in the visible light spectrum and the related transparent antenna exhibits microwave performance very close to the reference counterpart. On one hand, the use of a narrower pitch ($\lambda_0/300$) restricts strongly the optical transparency of the antenna (66%) while keeping up high microwave performance. On the other hand, the use of a wider pitch ($\lambda_0/30$) induces a slight increase of the optical transparency (89%), but affects both resonance frequency shift and gain values.

References

[1] T. Yasin, R. Baktur, and C. Furse, "A study on the efficiency of transparent patch antennas designed from conductive oxide films," *IEEE Int. Symp. Antennas and Propag.*, pp. 3085-3087, July 2011.

[2] F. Colombel et al., "Ultrathin metal layer, ITO film and ITO/Cu/ITO multilayer towards transparent antenna," *IET Sci. Meas. Technol.*, vol. 3, pp. 229-234, May 2009.

[3] T. Peter, T.I. Yuk, R. Nilavalan, and S.W. Cheung, "A novel technique to improve gain in transparent UWB antennas," in *Proc. Antennas and Propag. Conf. (LAPC)*, pp. 1-4, Nov. 2011.

[4] J. Hautcoeur, et al., "Transparency and electrical properties of meshed metal films," *Thin Solid Films*, vol. 519, pp. 3851-3858, March 2011.

[5] J. Hautcoeur, et al., "Optically transparent monopole antenna with high radiation efficiency manufactured with a silver grid layer (AgGL)", *Electron. Lett.*, vol. 45, pp.1014-1016, Sept. 2009.

[6] J. Hautcoeur, et al., "Comparison of the microwave performance of transparent wire monopole antennas based on silver films", *J. Electron. Mater.*, vol. 42, pp. 552-557, March 2013.

[7] Q.H. Dao, R. Braun, and B. Geck, "Design and investigation of meshed patch antennas for applications at 24 GHz," in *Proc. Eur. Microw. Week (EuMW)*, pp. 477-480, Sept. 2015.

[8] A. Martin, X. Castel, O. Lafond, and M. Himdi, "Optically transparent frequency-agile antenna for X-band applications," *Electron. Lett.*, vol. 51, pp. 1231–1233, August 2015.